

Photoelectron Angular Distributions for Two-photon Ionization of Helium by Ultrashort Extreme Ultraviolet Free Electron Laser Pulses

R. Ma,^{1,2,3} K. Motomura,^{1,2} K.L. Ishikawa,⁴ S. Mondal,^{1,2} H. Fukuzawa,^{1,2} A. Yamada,^{1,2} K. Ueda,^{1,2,*} K. Nagaya,^{2,5} S. Yase,^{2,5} Y. Mizoguchi,^{2,5} M. Yao,^{2,5} A. Rouzée,^{6,7} A. Hundermark,^{6,7} M.J.J. Vrakking,^{6,7} P. Johnsson,⁸ M. Nagasono,² K. Tono,² T. Togashi,^{2,9} Y. Senba,^{2,9} H. Ohashi,^{2,9} M. Yabashi,² and T. Ishikawa²

¹*Institute of Multidisciplinary Research for Advanced Materials, Tohoku University, Sendai 980-8577, Japan*

²*RIKEN, XFEL Project Head Office, Sayo, Hyogo 679-5148, Japan*

³*Institute of Atomic and Molecular Physics, Jilin University, Changchun 130012, China*

⁴*Photon Science Center, Graduate School of Engineering,*

The University of Tokyo, 7-3-1 Hongo, Bunkyo-ku, Tokyo 113-8656, Japan

⁵*Department of Physics, Kyoto University, Kyoto 606-8502, Japan*

⁶*Max-Born-Institut, Max-Born Strasse 2A, D-12489 Berlin, Germany*

⁷*FOM Institute AMOLF, Science park 102, 1098 XG Amsterdam, Netherlands*

⁸*Department of Physics, Lund University, 22100 Lund, Sweden*

⁹*Japan Synchrotron Radiation Research Institute, Sayo, Hyogo 679-5198, Japan*

(Dated: April 6, 2018)

Phase-shift differences and amplitude ratios of the outgoing s and d continuum wave packets generated by two-photon ionization of helium atoms are determined from the photoelectron angular distributions obtained using velocity map imaging. Helium atoms are ionized with ultrashort extreme-ultraviolet free-electron laser pulses with a photon energy of 20.3, 21.3, 23.0, and 24.3 eV, produced by the SPring-8 Compact SASE Source test accelerator. The measured values of the phase-shift differences are distinct from scattering phase-shift differences when the photon energy is tuned to an excited level or Rydberg manifold. The difference stems from the competition between resonant and non-resonant paths in two-photon ionization by ultrashort pulses. Since the competition can be controlled in principle by the pulse shape, the present results illustrate a new way to tailor the continuum wave packet.

PACS numbers: 32.80.Rm, 32.80.Fb, 41.60.Cr

Two-photon processes are well-known phenomena and have been extensively investigated for decades both experimentally and theoretically. Also these processes have been used in a variety of applications in laser optics and spectroscopy. It is well known that the two-photon photoelectron angular distributions are directly related to the relative amplitudes and the relative phase between different partial waves [1–6]. However, these earlier works dealt with the laser pulses in the optical range whose pulse width is very long in comparison with the modern standard of femosecond laser technology. The advent of extreme ultraviolet (EUV) [7, 8] and x-ray [9, 10] free-electron lasers (FELs), with femosecond pulse widths, has led to renewed interest in two-photon processes in the EUV to x-ray regimes (see, e.g., [11–19]). In the present Letter we address a new opportunity opened by the ultrashort EUV FEL pulses to deviate the phase shift difference between ionization channels from the scattering phase shift difference, which is otherwise intrinsic to the target atom or molecule. This will eventually open a new avenue to the coherent control of the continuum wave packets. (In this connection, see Ref. [20] for the control of the resonant two-color two-photon excitation yield and Ref [21] for the control of the photoelectron angular distributions of the nonperturbative resonant multi-photon ionization with ultrashort polarization-shaped pulses. See also a very recent review article for photo-

electron angular distributions [22].)

The simplest possible two-photon process may be (single-color) two-photon single ionization of helium atoms. For theoretical study, see, for example, the work by Nikolopoulos *et al.* [23], van der Hart and Bingham [24], and references cited therein. Kobayashi *et al.* [25] were the first to observe this process and used it for an autocorrelation measurement of high-order harmonic pulses, and Moshhammer *et al.* [26] recently used it for an autocorrelation measurement of the EUV FEL pulses provided by the SPring-8 Compact SASE Source (SCSS) test accelerator [8]. The absolute two-photon ionization cross sections of He were measured using an intense high harmonic source [27] as well as the SCSS test accelerator [28]. Hishikawa *et al.* [29] recently investigated two- and three-photon ionization of He at the SCSS test accelerator by photoelectron spectroscopy using a magnetic bottle spectrometer. The photoelectron angular distribution (PAD) for single-color two-photon ionization of helium, however, has not been investigated so far, though those from two-color two-photon (EUV + infrared) above-threshold ionization have recently been reported by Haber *et al.* [30].

Two-photon single ionization of helium produces a continuum electron wave packet which is a superposition of s and d partial waves. The photoelectron angular distribution provides information about the ratio of amplitudes

for the s and d partial waves and their relative phase. Extracting a phase shift difference from the PAD that is observed from a photoexcited state is a well-established method. For example, Haber *et al.* [31] excited the ground state helium atom to the $1snp$ Rydberg states by high-order harmonics and measured the PAD emitted from these excited states using IR and UV lasers as ionizing pulses. A similar experiment was also performed by O’Keeffe *et al.* [32] using synchrotron radiation for the excitation and a laboratory laser for the ionization. Both these experiments confirmed that the relative phase extracted from measured PADs resulting from sequential two-color excitation and ionization agrees well with the theoretically predicted scattering phase shift difference. In contrast, as theoretically predicted by Ishikawa and Ueda [33], the situation is significantly different for two-photon ionization by an intense short pulse as a competition between resonant and non-resonant ionization paths leads to a relative phase between s and d that is distinct from the corresponding scattering phase difference. It is expected that this change in the phase difference can be revealed by means of a PAD measurement.

In the present study, we use velocity map imaging (VMI) [34, 35] to measure the PAD from two-photon ionization of He by intense, femtosecond EUV FEL pulses. The anisotropy parameters are obtained from the PAD to extract the phase differences δ and the amplitude ratios of the s and d partial waves at four different photon energies ($\hbar\omega = 20.3, 21.3, 23.0,$ and 24.3 eV). Our results show the presence of an extra phase shift due to a competition between resonant and non-resonant paths, in agreement with our recent theoretical prediction [33] and simulation results obtained by solving the full time-dependent Schrödinger equation.

The experiments were carried out with the SCSS test accelerator in Japan. This FEL light source provided EUV pulses with a duration of ~ 30 fs [26] and a full-width-at-half-maximum spectral width of ~ 0.2 eV [36]. The photon energies were selected to be 20.3 eV, 21.3 eV, 23.0 eV, and 24.3 eV. A photon energy of 20.3 eV is well below the excitation energy to the lowest resonance $1s2p\ ^1P$ (21.218 eV) [37] and, thus, ionization is expected to be dominated by direct, non-resonant two-photon ionization. Photon energies 21.3 and 23.0 eV are close to the $1s2p\ ^1P$ and $1s3p\ ^1P$ (23.087 eV) [37] resonances. According to theoretical predictions [33], we may expect that competition between resonant and non-resonant paths can be seen. A photon energy of 24.3 eV corresponds to excitation to the $1snp\ ^1P$ Rydberg manifold ($n \sim 7$). The spectral width covers several Rydberg members from $1s6p\ ^1P$ to $1s9p\ ^1P$. In this condition we also expect that resonant and non-resonant ionization compete.

The FEL beam from the SCSS test accelerator was steered by two upstream plane SiC mirrors, passed a gas monitor detector (GMD), and then entered the prefocus-

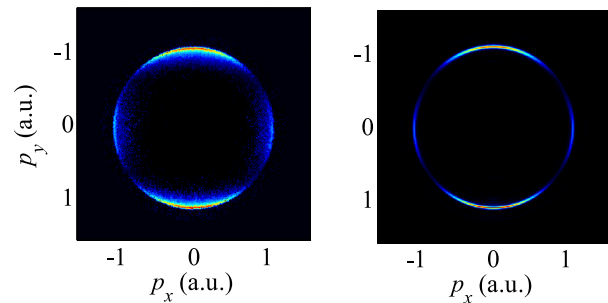


FIG. 1: Raw (left) and inverted (right) photoelectron images from two-photon ionization of helium at 20.3 eV photon energy.

ing system of the beam line. The GMD was calibrated using a cryogenic radiometer [38]. The average pulse energy measured by the GMD during the experiments was $7 - 11\ \mu\text{J}$, with a standard deviation of $2 - 4\ \mu\text{J}$. The focusing system, with a focal length of 1 m, consisted of a pair of elliptical and cylindrical mirrors coated with SiC [39]. The reflectivity of each mirror was 70 %. Before entering the interaction chamber, the FEL beam passed through two sets of light baffles, each consisting of three skimmers with 4.0 mm and 3.5 mm diameters, respectively. These baffles successfully removed the majority of the scattered light specularly and non-specularly reflected by the two mirrors, without reducing the photon flux. The FEL beam was then focused on a helium beam at the center of a VMI spectrometer [40]. The measured focal spot size was $\sim 13\ \mu\text{m}$ in radius, resulting in an average intensity of typically $2 - 3 \times 10^{13}\ \text{W}/\text{cm}^2$.

Electrons produced by two-photon ionization of the helium atoms by the FEL pulses were accelerated, perpendicularly to both the propagation and linear polarization axes of the FEL beam, towards a position-sensitive detector consisting of a set of microchannel plates (MCPs) followed by a phosphor screen. The positions of detected electrons were recorded using a gated CCD camera synchronized to the arrival of the FEL pulse in the interaction chamber. A 200 ns electrical gate pulse was applied to the back of the MCPs. The photoelectron angular distribution (PAD) has cylindrical symmetry along the FEL polarization, and we can retrieve the three-dimensional (3D) photoelectron momentum distribution from the raw two-dimensional (2D) image using a mathematical inversion procedure, which for each radial momentum leads to an expression of the photoelectron angular distribution in terms of Legendre coefficients (see Eq. (1) below). Examples of raw and inverted images are given in Fig. 1.

Figure 2 displays the PADs $I(\cos\theta)$ obtained at four different photon energies, as a function of cosine of the polar angle θ relative to the polarization axis. The PADs $I(\cos\theta)$ can be described by the following expression:

$$I(\cos\theta) = \frac{I_0}{4\pi} [1 + \beta_2 P_2(\cos\theta) + \beta_4 P_4(\cos\theta)] , \quad (1)$$

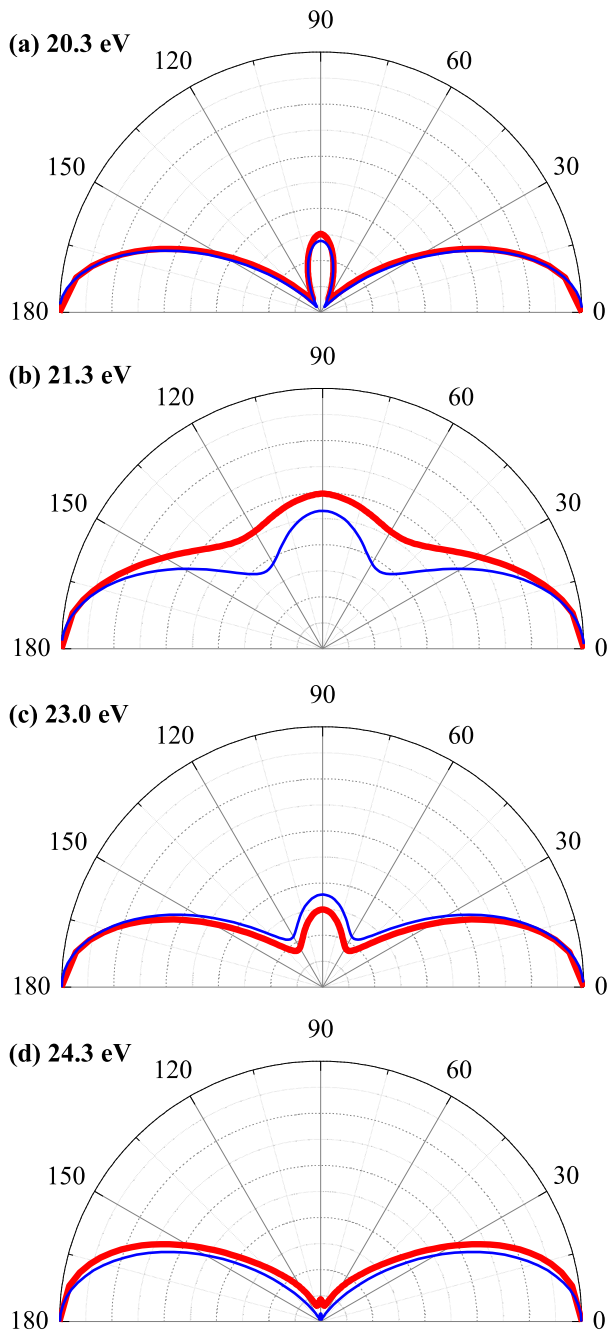


FIG. 2: (Color online) Measured (thick red lines) and calculated (thin blue lines) photoelectron angular distributions for two-photon ionization of helium at photon energies of 20.3, 21.3, 23.0, and 24.3 eV.

TABLE I: Experimentally obtained anisotropy parameters β_2 and β_4 , and the extracted values of W and Δ .

$\hbar\omega$ (eV)	β_2	β_4	W	Δ
20.3	1.14 ± 0.07	1.96 ± 0.03	0.561 ± 0.016	1.60 ± 0.05
21.3	0.268 ± 0.019	0.384 ± 0.063	2.39 ± 0.23	1.61 ± 0.04
23.0	0.948 ± 0.010	1.32 ± 0.15	0.977 ± 0.116	1.67 ± 0.04
24.3	2.11 ± 0.10	0.841 ± 0.006	1.43 ± 0.01	2.47 ± 0.07

where I_0 is the angle-integrated intensity, β_2 and β_4 are the anisotropy parameters associated with the second- and fourth-order Legendre polynomials $P_2(x)$ and $P_4(x)$, respectively. Values of β_2 and β_4 obtained from the experimental PADs are listed in Table 1.

To investigate the processes involved in the two photon ionization of He, we have performed numerical simulations, by solving the full-dimensional two-electron time-dependent Schrödinger equation (TDSE) using the time-dependent close-coupling method [41–45]. We have employed chaotic pulses with a mean intensity of $2.5 \times 10^{13} \text{ W/cm}^2$, generated by the partial-coherence method described in Ref. [46], for a coherence time of 8 fs and a mean pulse width of 28 fs (full width at half maximum), as recently measured by second-order autocorrelation [26], both assumed to have Gaussian profiles on average. One can see a good agreement between the experimental and simulation results in Fig. 2 as well as in Fig. 3 below.

The PAD results from an interference of the s and d partial waves, and can be expressed as,

$$\begin{aligned} &\propto |c_0 e^{i\delta_{sc,0}} Y_{00} - c_2 e^{i\delta_{sc,2}} Y_{20}|^2 \\ &= ||c_0| e^{i\delta_0} Y_{00} - |c_2| e^{i\delta_2} Y_{20}|^2, \end{aligned} \quad (2)$$

where c_l denotes the complex amplitude of a final state with an angular momentum l , $\delta_{sc,l}$ the scattering phase shift intrinsic to the corresponding continuum eigen function, and $\delta_l = \arg c_l + \delta_{sc,l}$ the phase of each partial wave. If we define $W = |c_0/c_2|$ and $\Delta = \delta_0 - \delta_2$, then, these are related to the anisotropy parameters as,

$$\beta_2 = \frac{10}{W^2 + 1} \left[\frac{1}{7} - \frac{W}{\sqrt{5}} \cos \Delta \right], \quad \beta_4 = \frac{18}{7(W^2 + 1)}, \quad (3)$$

and thus W and δ can be extracted from the PAD. The experimentally obtained values of W and Δ are listed in Table I. Furthermore, the experimental values of W and Δ are compared with values extracted from TDSE simulations in Fig. 3 as a function of photon energy $\hbar\omega$. The agreement between experimental and theoretical values are reasonable for both W and Δ . For comparison, theoretical values of the scattering phase shift difference $\Delta_{sc} \equiv \delta_{sc,0} - \delta_{sc,2}$ [47] are also plotted by the solid line.

Within the framework of the second-order time-dependent perturbation theory [33], c_l can be defined in such a way that its real and imaginary parts correspond to the resonant and non-resonant paths, respectively. If the pulse is non-resonant, c_0 and c_2 are pure imaginary, resulting in $\Delta = \Delta_{sc}$. In the present study, the measurement at $\hbar\omega = 20.3 \text{ eV}$ corresponds to this situation; indeed, we find $\Delta \approx \Delta_{sc}$ in this case in Fig. 3.

Let us now turn to the situation where the pulse is resonant with an excited state or Rydberg manifold. If a resonant two-photon ionization path is dominant, Δ is again close to Δ_{sc} , since c_0 and c_2 are both real. On the

other hand, if the contributions from both the resonant (via a single or several resonant levels) and non-resonant paths (via all the intermediate levels) are present, then $\Delta \neq \Delta_{sc}$ in general [33] and an extra phase shift difference $\Delta_{ex} \equiv \Delta - \Delta_{sc} = \arg c_0/c_2$ occurs that can be viewed as a measure of the competition between them. In the present study, the pulses with $\hbar\omega = 21.3, 23.0,$ and 24.3 eV induce resonant two-photon ionization via $1s2p^1P, 1s3p^1P,$ and a Rydberg manifold ($1snp^1P$ with $n = 6 - 9$), respectively. We can see in Fig. 3 that the relative phase Δ deviates from the scattering phase shift difference Δ_{sc} for these three photon energies; the difference Δ_{ex} increases gradually with increasing photon energy and becomes very significant at 24.3 eV. At $\hbar\omega = 21.3$ and 23.0 eV, the simulation values of Δ_{ex} are slightly smaller than for lower intensity, indicating the departure from the perturbative limit due to the high intensity. The observed deviation Δ_{ex} clearly demonstrates the presence of a competition between resonant and non-resonant paths in the present experiments, as recently predicted in Ref. [33]. This situation presents a contrast to the case of the photoionization from excited p states [31, 32], where the non-resonant path is absent and, as a result, $\Delta = \Delta_{sc}$. Although the competition has been implicitly used in coherent control of resonance-enhanced multi-photon processes (see, e.g., [20, 21]), intermediate levels other than the resonant level are neglected in most cases. In the present study, on the other hand, the contribution from non-resonant intermediate levels is essential to account for Δ_{ex} [33], which explains why Δ_{ex} is larger for a higher photon energy, i.e., for smaller level spacing.

It may be worth pointing out the similarity between two-photon ionization via a Rydberg manifold and two-photon above-threshold ionization. In the case of the 24.3 eV excitation, the intense ultrashort EUV pulses used in the present study coherently excite several Rydberg states $1snp^1P$ with $n = 6 - 9$. In such a situation, the Rydberg manifold behaves similarly to the continuum near the threshold and both the relative phase Δ [33] and the TPI yield [48] would smoothly vary when measured by increasing the photon energy across the ionization threshold. It should be noted that the extra phase shift difference due to free-free transitions plays a significant role in recently observed time delays in photoemission by attosecond EUV pulses [49, 50].

In conclusion, we have measured the PAD from two-photon ionization of He by intense, femtosecond EUV FEL pulses provided by the SCSS test accelerator in Japan using a VMI spectrometer. From the anisotropy parameters of the PAD, we extracted phase-shift differences Δ and amplitude ratios W of the s and d partial waves at four different photon energies ($\hbar\omega = 20.3, 21.3, 23.0,$ and 24.3 eV). As a result, we have demonstrated that competition between resonant and non-resonant processes in two-photon ionization by intense femtosecond pulses causes an additional phase shift in

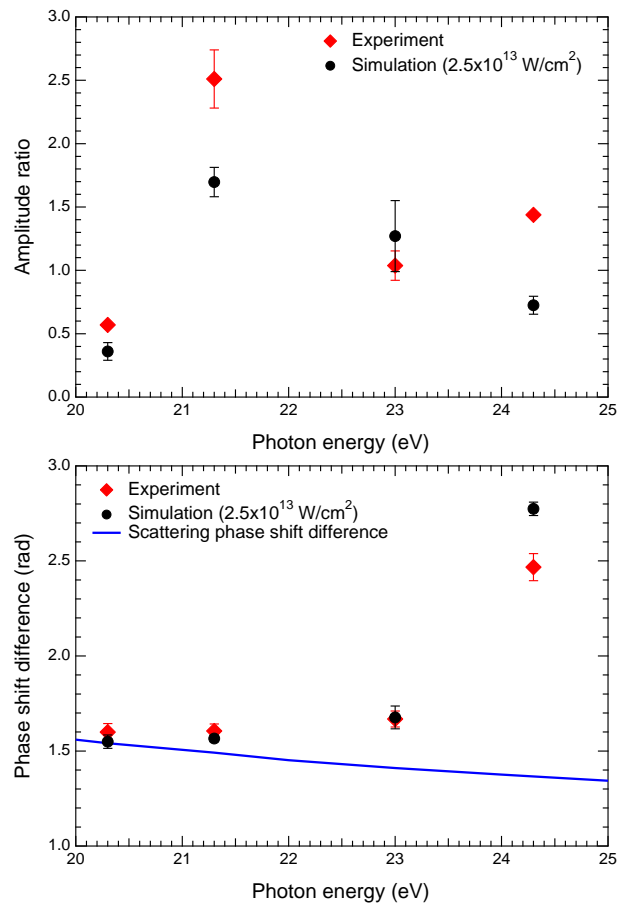


FIG. 3: (Color online) Amplitude ratio W (upper panel) and phase shift difference (relative phase) Δ (lower panel) extracted from experimental and theoretical PADs. Theoretical scattering phase shift difference Δ_{sc} [47] is also included in the lower panel.

the photoelectron wavepacket. The competition can in principle be controlled by chirping the EUV pulses, which may pave a way to tailor continuum wave packets. Such an experiment will become feasible in the near future at FEL facilities where the pulses can be controlled in the range of a few to a few tens of fs.

We are grateful to the SCSS Test Accelerator Operation Group at RIKEN for continuous support in the course of the studies and to the staff of the technical service section in IMRAM, Tohoku University, for their assistance in constructing the apparatus. This study was supported by the X-ray Free Electron Laser Utilization Research Project of the Ministry of Education, Culture, Sports, Science and Technology of Japan (MEXT), by the Management Expenses Grants for National Universities Corporations from MEXT, by Grants-in-Aid for Scientific Research from JSPS (No. 21244062 and No. 22740264), and IMRAM research program. K.L.I. gratefully acknowledges support by the APSA Project (Japan), KAKENHI (No. 23656043 and No.

23104708), the Project of Knowledge Innovation Program (PKIP) of Chinese Academy of Sciences (Project No. KJCX2.YW.W10), and the Cooperative Research Program of Network Joint Research Center for Materials and Devices. The research of A.H., A.R. and M.V. is part of the research program of the “Stichting voor Fundamenteel Onderzoek der Materie (FOM)”, which is financially supported by the “Nederlandse organisatie voor Wetenschappelijk Onderzoek (NWO)”. P.J. acknowledges support from the Swedish Research Council and the Swedish Foundation for Strategic Research.

* ueda@tagen.tohoku.ac.jp

- [1] S.N. Dixit and P. Lambropoulos, **27**, 861 (1983).
- [2] S.J. Smith, G. Leuchs Adv. At. Mol. Phys. **24**, 157-221 (1988).
- [3] P. Lambropoulos, P. Maragikis, and J. Zhang, Phys. Rep. **305**, 203 (1998).
- [4] Z.-M. Wang and D.S. Elliott, Phys. Rev. Lett. **87**, 173001 (2001).
- [5] K.L. Reid, Annu. Rev. Chem. **54**, 397 (2003).
- [6] N.M. Kabachnik, S. Fritzsche, A.N. Grum-Grzhimailo, M. Meyer, and K. Ueda, Phys. Rep. **451**, 155 (2007).
- [7] W. Ackermann *et al.*, Nat. Photonics, **1**, 336 (2007).
- [8] T. Shintake *et al.*, Nat. Photonics, **2**, 555 (2008).
- [9] P. Emma *et al.*, Nat. Photonics, **4**, 641 (2010).
- [10] T. Ishikawa *et al.*, Nat. Photonics **6**, 540 (2012).
- [11] M. Nagasono *et al.*, Phys. Rev. A **75**, 051406 (2007).
- [12] H. R. Varma, M. F. Ciappina, N. Rohringer, and R. Santra, Phys. Rev. A **80**, 053424 (2009).
- [13] R. Santra, N. V. Kryzhevoi, and L. S. Cederbaum, Phys. Rev. Lett. **103**, 013002 (2009).
- [14] L. Young *et al.*, Nature (London) **466**, 56 (2010).
- [15] J..P. Cryan *et al.*, Phys. Rev. Lett. **105**, 083004 (2010).
- [16] L. Fang *et al.*, Phys. Rev. Lett. **105**, 083005 (2010).
- [17] N. Berrah *et al.*, Proc. Nat. Acad. Sci. **108**, 16912 (2011).
- [18] G. Doumy *et al.*, Phys. Rev. Lett. **106**, 083002 (2011).
- [19] P. Salén *et al.*, Phys. Rev. Lett. **108**, 153003 (2012).
- [20] N. Dudovich, B. Dayan, S.M. Gallagher Faeder, and Y. Silberberg, Phys. Rev. Lett. **86**, 47 (2001).
- [21] M. Wollenhapt M. Klug, J. Köhler, T. Bayer, C. Sarpe-Tudoran, and T. Baumert, Appl. Phys. B **95**, 245 (2009).
- [22] K.L. Reid, Mol. Phys. **110**, 131 (2012).
- [23] L.A.A. Nikolopoulos and P. Lambropoulos, J. Phys. B: At. Mol. Opt. Phys. **34**, 545 (2001).
- [24] H.W. van der Hart and P. Bingham, J. Phys. B: At. Mol. Opt. Phys. **38**, 207 (2005).
- [25] Y. Kobayashi, T. Sekikawa, Y. Nabekawa, and S. Watanabe, Opt. Lett. **23**, 64 (1998).
- [26] R. Moshhammer *et al.*, Opt. Express **19**, 21698 (2011).
- [27] H. Hasegawa, E. J. Takahashi, Y. Nabekawa, K. L. Ishikawa, and K. Midorikawa, Phys. Rev. A **71**, 023407 (2005).
- [28] T. Sato *et al.*, J. Phys. B: At. Mol. Opt. Phys. **44**, 161001 (2011).
- [29] A. Hishikawa *et al.*, Phys. Rev. Lett. **107**, 243003 (2011).
- [30] L. H. Haber, B. Doughty, and S. R. Leone, Phys. Rev. A **84**, 013416 (2011).
- [31] L. H. Haber, B. Doughty, and S. R. Leone, Phys. Rev. A **79**, 031401(R) (2009).
- [32] P. O’Keeffe P. Bolognesi, R. Richter, A. Moise, E. Ovcharenko, L. Pravica, R. Sergo, L. Stebel, G. Cautero, and L. Avaldi1, J. Phys.: Conf. Ser. **235**, 012006 (2010).
- [33] K.L. Ishikawa and K. Ueda, Phys. Rev. Lett. **108**, 033003 (2012).
- [34] A. T. J. B. Eppink and D. H. Parker, Rev. Sci. Instrum. **68**, 3477 (1997).
- [35] A. Rouzee *et al.*, Phys. Rev. A **83**, 031401(R) (2011).
- [36] Y. Hikosaka *et al.*, Phys. Rev. Lett. **105**, 133001 (2010).
- [37] http://physics.nist.gov/PhysRefData/ASD/levels_form.html.
- [38] M. Kato *et al.*, Nucl. Instrum. Methods Phys. Res. A **612**, 209 (2009).
- [39] H. Ohashi *et al.*, Nucl. Instrum. Methods Phys. Res., Sect. A **649**, 58 (2011).
- [40] E.V. Gryzlova *et al.*, Phys. Rev. A **84**, 063405 (2011).
- [41] M. S. Pindzola and F. Robicheaux, Phys. Rev. A **57**, 318 (1998).
- [42] M. S. Pindzola and F. Robicheaux, J. Phys. B **31**, L823 (1998).
- [43] J. Colgan, M. S. Pindzola, and F. Robicheaux, J. Phys. B **34**, L457 (2001).
- [44] J. S. Parker, L. R. Moore, K. J. Meharg, D. Dundas, and K. T. Taylor, J. Phys. B **34**, L69 (2001).
- [45] K. L. Ishikawa and K. Midorikawa, Phys. Rev. A **72**, 013407 (2005).
- [46] T. Pfeifer, Y. Jiang, S. Düsterer, R. Moshhammer, and J. Ullrich, Opt. Lett. **35**, 3441 (2010).
- [47] T. T. Gien, J. Phys. B **35**, 4475 (2002).
- [48] K. L. Ishikawa, Y. Kawazura, and K. Ueda, J. Mod. Opt. **57**, 999 (2010).
- [49] M. Schultze *et al.*, Science **328**, 1658 (2010).
- [50] K. Klünder *et al.*, Phys. Rev. Lett. **106**, 143002 (2011).